



Queensland University of Technology
Brisbane Australia

This is the author's version of a work that was submitted/accepted for publication in the following source:

[Ilic, Milos](#) (2014) *Images inside a reflecting spherical surface with possible application in astronomy*. [Working Paper] (Unpublished)

This file was downloaded from: <http://eprints.qut.edu.au/73207/>

© Copyright 2014 The Author

Notice: *Changes introduced as a result of publishing processes such as copy-editing and formatting may not be reflected in this document. For a definitive version of this work, please refer to the published source:*

Images inside a Reflecting Spherical Surface with possible Application in Astronomy

M. Ilić

Mathematical Sciences, Queensland University of Technology

P.O.B. 2434, Brisbane, Qld 4001, Australia

Email: m.ilic@qut.edu.au

Abstract

This report studies an algebraic equation whose solution gives the image system of a source of light as seen by an observer inside a reflecting spherical surface. The equation is looked at numerically using GeoGebra. Under the hypothesis that our galaxy is enveloped by a reflecting interface this becomes a possible model for many mysterious extra galactic observations.

1 Introduction

The image system produced by two mirrors on the opposite parallel walls is striking and easily explained using the well known Snell's reflection laws. In a nutshell, the image system of a source of light within a parallel strip (two parallel reflecting planes) as seen by an observer also within the strip consists of an infinity of images on either side of the strip on a line which passes through the source and is perpendicular to the strip. It is not hard to obtain equations (or geometrically) that give the positions of these images. Now suppose we find ourselves inside a sphere which has a reflecting surface, what would we see?

Reflection from spherical mirrors of small aperture is studied in secondary schools. Study of images inside a reflecting spherical surface is much more challenging and seems to have escaped the attention of students of optics. The problem can be considerably simplified by noting that all the action occurs in the plane containing the source S , the observer P and the centre of the sphere O or more precisely inside the great circle \mathcal{C} formed by this plane and the sphere. For any ray of light from S to reach P , it must travel in the plane OPS directly from S to P or by reflections from the circle \mathcal{C} . Any tangent to \mathcal{C} acts as a mirror and is perpendicular to the radius. From symmetry the results obtained for this plane can be applied to any other source by rotating the plane about the line OP . Our problem becomes: Find all images of a source S at (r, θ) (in polar coordinates) as seen by an observer P on the x -axis, at $(h, 0)$ inside a circle centre O and radius R . Figure 1 shows a ray going clockwise with reflection points A_1, A_2, \dots , where

A_n is (R, ω_n) in polar coordinates. Figure 2 shows a ray going anticlockwise with reflection points B_1, B_2, \dots , where B_n is (R, ν_n) .

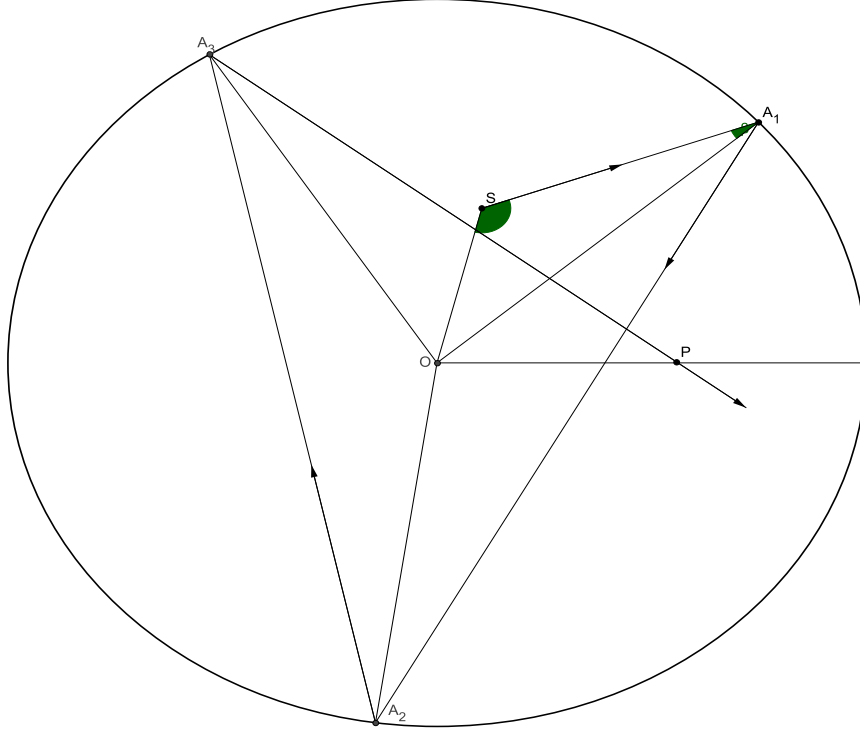


Fig. 1 Clockwise Ray

In Section 2 we derive an algebraic equation whose solution gives the image system. Section 3 is devoted to analytical considerations and Section 4 to numerical discussion using GeoGebra [1]. The images are classified into categories depending on the number of reflections: zero for the direct ray; then as first, second, \dots category depending on how many times the ray is reflected from \mathcal{C} before reaching P. Using continuity of our equations we can conclude that an extended source (or a cluster of sources) produces an extended image (or a cluster of images) in a given category.

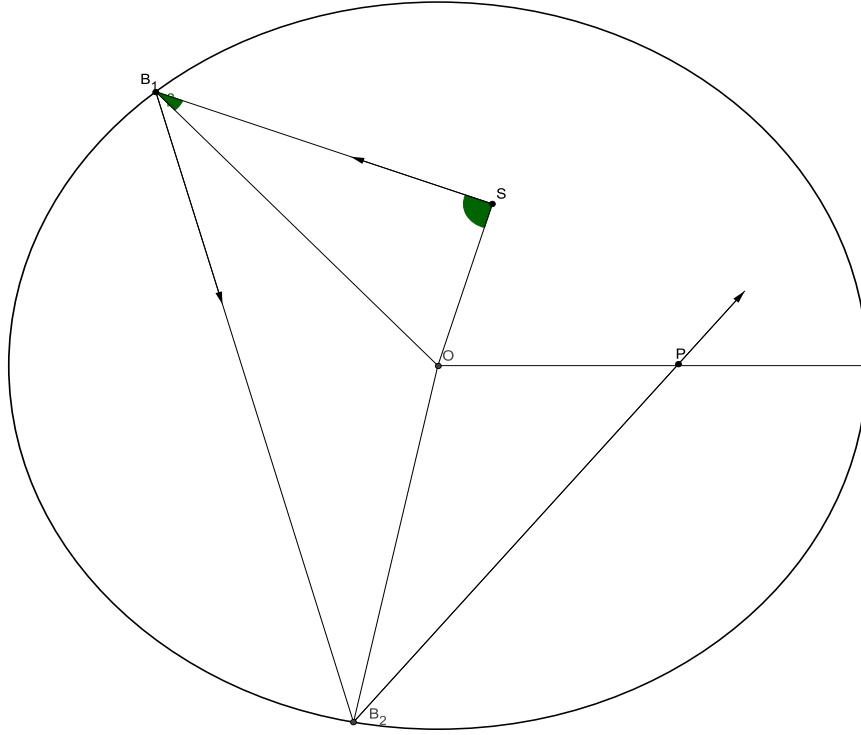


Fig.2 Anticlockwise Ray

At this stage the reader may be asking the question: Could there be any possible application of the above model? An amateur astronomer reading recent popular articles on astronomy can't help being puzzled by different theories to explain many mysterious observations. We come across billions of galaxies moving at near speed of light, walls of galaxies, dark matter, quantized red shifts, laws of gravity not holding at the edge of our Milky Way galaxy etc. In essence this report proposes that our galaxy, the Milky Way, is bounded by a reflecting interface. At this stage I have no proof that it exists but, as usual in mathematical modelling, it can be proved as appropriate or not by professional astronomers using the modern equipment. As a first step in the search for a proof, Section 5 looks at the position of known galaxies and their possible sources. Since for an amateur astronomer it is not obvious which 'sources' (stars, clusters etc) are primary or which are images, it is reasonable to assume that 'galaxies' are images. Hence if the model can get off the ground LMC, SMC, Andromeda and the other galaxies are reflected images whose sources are at or near the centre of the Milky Way. In fact most of the Milky Way 'cloud' can be considered as a reflection rather than having to introduce 'new outer arms' to account for observed phenomenon.

Considerations in Section 5 yielded an unexpected result that the centre

of the galaxy may not be the centre of the spherical surface. The centre of the galaxy may be at the focus of an ellipsoidal surface. This is briefly looked at in Section 6. Finally, some conclusions are drawn in Section 7.

2 Derivation of the *Image* Equation

To derive the image system of a source at $S(r, \theta)$, where $0 < \theta < 2\pi$, and the observer is at $P(h, 0)$, it is best to consider clockwise and anticlockwise rays separately, since the former arrives from $y > 0$ direction and the latter from $y < 0$ direction.

1. Clockwise Ray

In Figure 1 in Section 1, let $\angle OSA_1 = \alpha$ and $\angle SA_1O = \beta$. Then

$$\angle OA_1A_2 = \beta,$$

since the angle of incidence is equal to the angle of reflection. Also

$$\angle OA_2A_1 = \beta,$$

since $\triangle OA_1A_2$ is an isosceles triangle. Clearly

$$\omega_1 = \theta + \alpha + \beta - \pi, \quad \omega_2 = \omega_1 - (\pi - 2\beta),$$

and in general for $n = 1, 2, \dots$

$$\begin{aligned} \omega_n &= \omega_{n-1} - (\pi - 2\beta) \\ &= \omega_1 - (n-1)(\pi - 2\beta) \\ &= \theta + \alpha + (2n-1)\beta - n\pi. \end{aligned}$$

Cartesian coordinates for A_n are $(R \cos(\omega_n), R \sin(\omega_n))$. Straight line A_nA_{n+1} is

$$\begin{aligned} \frac{y - R \sin(\omega_n)}{x - R \cos(\omega_n)} &= \frac{R \sin(\omega_{n+1}) - R \sin(\omega_n)}{R \cos(\omega_{n+1}) - R \cos(\omega_n)} \\ &= \frac{\sin(\omega_{n+1}) - \sin(\omega_n)}{\cos(\omega_{n+1}) - \cos(\omega_n)} \\ &= \frac{2 \cos\left\{\frac{\omega_{n+1} + \omega_n}{2}\right\} \sin\left\{\frac{\omega_{n+1} - \omega_n}{2}\right\}}{-2 \sin\left\{\frac{\omega_{n+1} + \omega_n}{2}\right\} \sin\left\{\frac{\omega_{n+1} - \omega_n}{2}\right\}} \\ &= \frac{\sin(\omega_n + \beta)}{\cos(\omega_n + \beta)}, \end{aligned}$$

using trigonometric formulae. Hence

$$y \cos(\omega_n + \beta) - x \sin(\omega_n + \beta) = -R \sin(\beta).$$

For this line to pass through $P(x = h, y = 0)$, we have

$$b \sin(\omega_n + \beta) = \sin(\beta), \quad (1)$$

where $b = \frac{h}{R}$. Sine Rule for the $\triangle OSA_1$ gives $\frac{R}{\sin(\alpha)} = \frac{r}{\sin(\beta)}$, i.e.

$$a \sin(\alpha) = \sin(\beta), \quad (2)$$

where $a = \frac{r}{R}$. Equations (1) and (2) define α and β . We prefer to use the *angle of sight* ϕ i.e the angle that the vector $P\vec{A}_n$ makes with the positive x -axis. Sine Rule for the $\triangle OPA_n$ gives $\frac{R}{\sin(\pi-\phi)} = \frac{h}{\sin(\beta)}$, i.e.

$$b \sin(\phi) = \sin(\beta). \quad (3)$$

Combining equations (1) and (3), we have

$$\begin{aligned} 0 &= \sin(\omega_n + \beta) - \sin(\phi) \\ &= 2 \cos\left\{\frac{\omega_n + \beta + \phi}{2}\right\} \sin\left\{\frac{\omega_n + \beta - \phi}{2}\right\} \\ &= 2 \cos\left\{\frac{\theta + \alpha + 2n\beta - n\pi + \phi}{2}\right\} \sin\left\{\frac{\theta + \alpha + 2n\beta - n\pi - \phi}{2}\right\}. \end{aligned}$$

From which we conclude that $\theta + \alpha + 2n\beta - n\pi + \phi = (2m + 1)\pi$ or $\theta + \alpha + 2n\beta - n\pi - \phi = 2m\pi$, where $m = 0, \pm 1, \pm 2, \dots$. For $n = 1$, these become $\theta + \alpha + 2\beta - \pi + \phi = (2m + 1)\pi$ and $\theta + \alpha + 2\beta - \pi - \phi = 2m\pi$. From Figure 1, the angle ϕ in the former is the angle $\angle OPA_1$, the ϕ in the latter is its supplement i.e. the angle of sight as defined previously. For consistency we take

$$\theta + \alpha + 2n\beta - n\pi - \phi = 2m\pi. \quad (4)$$

Using equations (2), (3) and (4) and eliminating α and β , we obtain the *image equation* for clockwise rays as

$$b \sin(\phi) + (-1)^n a \sin\{2n \arcsin(b \sin(\phi)) - \phi + \theta\} = 0, \quad (CR)$$

where $0 < a < 1$, $0 < b < 1$, $0 < \theta < 2\pi$ and $0 < \phi < \pi$.

2. Anticlockwise Ray

In Figure 2 in Section 1, let $\angle OSB_1 = \alpha$ and $\angle SB_1O = \beta$. Then $\angle OB_1B_2 = \beta$, and $\angle OB_2B_1 = \beta$ as before. Clearly

$$\nu_1 = \theta - \alpha - \beta + \pi, \quad \nu_2 = \nu_1 + (\pi - 2\beta),$$

and in general for $n = 1, 2, \dots$

$$\begin{aligned} \nu_n &= \nu_{n-1} + (\pi - 2\beta) \\ &= \nu_1 + (n-1)(\pi - 2\beta) \\ &= \theta - \alpha - (2n-1)\beta + n\pi. \end{aligned}$$

Cartesian coordinates for B_n are $(R \cos(\nu_n), R \sin(\nu_n))$. One can write the straight line $B_n B_{n+1}$ as before, which on simplification becomes

$$y \cos(\nu_n - \beta) - x \sin(\nu_n - \beta) = R \sin(\beta).$$

For this line to pass through $P(x = h, y = 0)$, we have

$$b \sin(\nu_n - \beta) + \sin(\beta) = 0. \quad (5)$$

Application of the Sine Rule for the $\triangle OSB_1$ and the $\triangle OPB_n$ gives $a \sin(\alpha) = \sin(\beta)$ and $b \sin(\phi) = \sin(\beta)$, respectively. Proceeding as before, we obtain the *image equation* for anticlockwise rays as

$$b \sin(\phi) + (-1)^n a \sin\{2n \arcsin(b \sin(\phi)) - \phi - \theta\} = 0, \quad (AR)$$

where $0 < a < 1$, $0 < b < 1$, $0 < \theta < 2\pi$ and $0 < \phi < \pi$.

3 Analytical Considerations

First we note that if we set $\theta = \bar{\theta} + 2\pi$, then (CR) and (AR) equations don't change, only θ is replaced by $\bar{\theta}$. This allows us to take $-\pi < \theta < \pi$ instead of $0 < \theta < 2\pi$. If we allow ϕ to take negative values i.e. if we set $\phi = -\bar{\phi}$ in (CR) we obtain (AR). In other words (CR) and (AR) can be combined in a single equation

$$b \sin(\phi) + (-1)^n a \sin\{2n \arcsin(b \sin(\phi)) - \phi + \theta\} = 0, \quad (IE)$$

where $0 < a < 1$, $0 < b < 1$, $-\pi < \theta < \pi$ and $-\pi < \phi < \pi$, $n = 1, 2, \dots$, where $\phi > 0$ corresponds to the images formed by the clockwise rays and $\phi < 0$ for anticlockwise images for a given source.

Let $D = \{(\phi, \theta, a, b) | -\pi < \phi < \pi, -\pi < \theta < \pi, 0 < a < 1, 0 < b < 1\}$ and define $F_n : D \rightarrow R$, $n = 1, 2, \dots$ by

$$F_n(\phi, \theta, a, b) = b \sin(\phi) + (-1)^n a \sin\{2n \arcsin(b \sin(\phi)) - \phi + \theta\}.$$

Then all the informatin about the images can be obtained by studying the equation $F_n = 0$ on D . Noting that n refers to how many times the ray is reflected before reaching the observer, we classify the images into categories depending on n : zero for the direct ray; then as first, second, \dots category for $n = 1, 2, \dots$ respectively. In this report we shall not examine the complete structure for all n ; rather we look at the images within a given category i.e. n is considered as fixed and F_n will be taken as F , and subscript notation will be used for partial derivatives. For example $F_\phi = \frac{\partial F}{\partial \phi}$.

Solutions of (IE)

Clearly one cannot solve (IE) explicitly. Here we summarise a few obvious results:

1. *Solution by Inspection* We mention a number of cases:

- (a) If $a = 0$ i.e. the source is at the centre ($b \neq 0$), then $\phi = 0$ (reflected ray on observer's side) or $\phi = \pi$ (reflected clockwise ray on the other side) or $\phi = -\pi$ (reflected anticlockwise ray on the other side), for all n .
- (b) If $b = 0$ i.e. the observer is at the centre ($a \neq 0$), then $\phi = \theta$ or $\phi = \theta + \pi$ which are the rays along the diameter along OS, for all n .
- (c) If $\theta = 0$ ($a \neq 0, b \neq 0$), then $\phi = 0$ (reflected ray on observer's side) or $\phi = \pi$ (reflected clockwise ray on the other side) or $\phi = -\pi$ (reflected anticlockwise ray on the other side), for all n .
- (d) If $\theta = \pi$ or $-\pi$ ($a \neq 0, b \neq 0$), then $\phi = 0$ (reflected ray on observer's side) or $\phi = \pi$ (reflected clockwise ray on the other side) or $\phi = -\pi$ (reflected anticlockwise ray on the other side), for all n .

2. *Numerical Solution* To find the solutions of (IE) for ϕ in terms of the other variables, we need numerical methods which will be discussed in the next section.

3. *Cluster of Sources or Extended Source* The equation $F(\phi, \theta, a, b) = 0$ defines ϕ implicitly in terms of other variables. Clearly F is continu-

ously differentiable in D with partial derivatives

$$\begin{aligned} F_\phi &= b \cos(\phi) + (-1)^n a \cos\{2n \arcsin(b \sin(\phi)) - \phi + \theta\} \\ &\quad + \theta \left\{ \frac{2nb \cos(\phi)}{\sqrt{1 - b^2 \sin^2(\phi)}} - 1 \right\}, \\ F_\theta &= (-1)^n a \cos\{2n \arcsin(b \sin(\phi)) - \phi + \theta\}, \\ F_a &= (-1)^n \sin\{2n \arcsin(b \sin(\phi)) - \phi + \theta\}, \\ F_b &= \sin(\phi). \end{aligned}$$

Since $b < 1$, $(1 - b^2 \sin^2(\phi)) > 0$.

Suppose that for a given $\hat{z} = (\theta, a, b)$ and n , we obtain (numerically) ϕ_0 i.e. $F(\phi_0, \hat{z}) = 0$ and $F_\phi(\phi_0, \hat{z}) \neq 0$. The Implicit Function Theorem of Multivariable Calculus states that there exists a unique function $f(\theta, a, b)$ and a neighbourhood N of \hat{z} such that $\phi = f(\hat{z})$, $F(f(\theta, a, b), \theta, a, b) = 0$, for $(\theta, a, b) \in N$ and $f \in C^1$, $(\theta, a, b) \in N$. The partial derivatives of $\phi = f$ are

$$\frac{\partial \phi}{\partial \theta} = -\frac{F_\theta}{F_\phi}, \quad \frac{\partial \phi}{\partial a} = -\frac{F_a}{F_\phi}, \quad \frac{\partial \phi}{\partial b} = -\frac{F_b}{F_\phi}.$$

The meaning of this mathematical result is that the neighbourhood N can represent a cluster of sources or an extended (not just a point) source. The critical condition is that $F_\phi \neq 0$.

4. *Variation in Parameters* The usual error estimation formula can be applied viz

$$\delta(\phi) = \frac{\partial \phi}{\partial \theta} \delta(\theta) + \frac{\partial \phi}{\partial a} \delta(a) + \frac{\partial \phi}{\partial b} \delta(b).$$

to see the effect of displacing the source or the observer.

5. *Distribution of Sources for a given ϕ* Suppose we fix the position of the observer $b = \text{constant}$ and the angle of sight i.e. $\phi = \text{constant}$, the equation (IE) gives a relation between a and θ i.e. the distribution of sources that give the same ϕ . One easily obtains

$$\begin{aligned} a &= \frac{(-1)^{n+1} b \sin(\phi)}{\sin\{2n \arcsin(b \sin(\phi)) - \phi + \theta\}} \\ &= (-1)^{n+1} b \sin(\phi) \csc\{2n \arcsin(b \sin(\phi)) - \phi + \theta\}, \end{aligned} \quad (6)$$

$0 < a < 1$.

This was graphed using GeoGebra by setting $S = (a \cos(\theta), a \sin(\theta))$ and using sliders for ϕ, θ and n . One can show that all the values of

(a, θ) lie on the straight lines, the incident rays, as depicted in Figure 3 for clockwise rays for category 1 sources $n = 1$ (black), category 2 $n = 2$ (red), category 3 $n = 3$ (blue) and category 4 $n = 4$ (green).

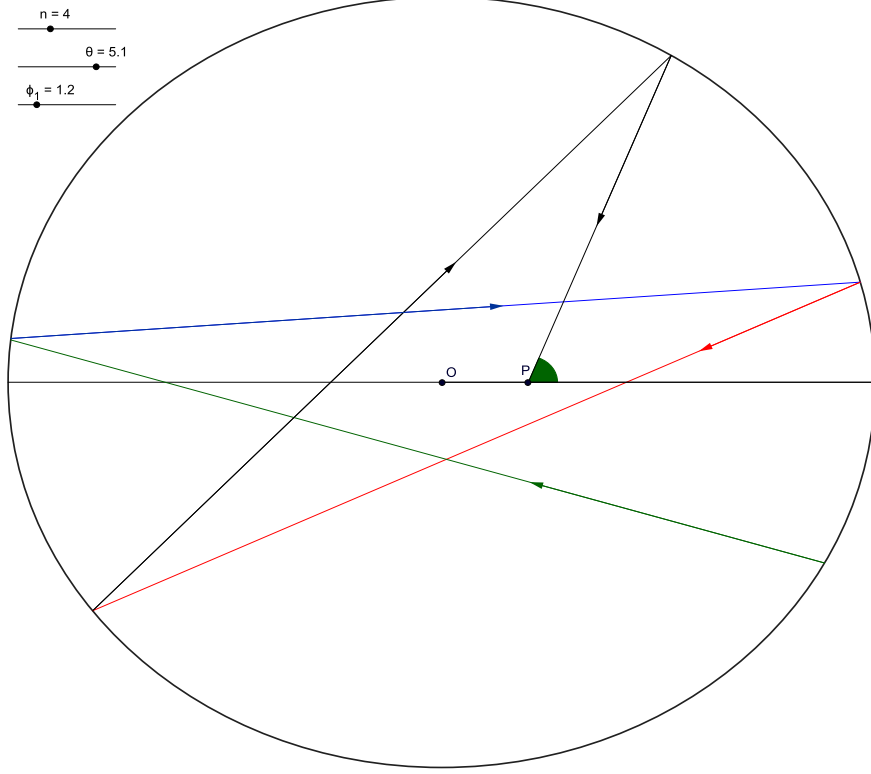


Fig.3 Possible sources for a given ϕ

4 Numerical Solution

As mentioned in the last section, to solve (IE) for ϕ we need a numerical method. One option is to use GeoGebra which is an interactive mathematics software that joins geometry, algebra and calculus. One can construct objects like the figures in this paper and plot graphs of functions such as

$$Y = F(\phi, \theta, a, b),$$

where θ, a, b are treated as parameters which can be varied continuously by using so called 'sliders'. It is a simple task to obtain the root (or roots) in any given interval by specifying upper and lower limits of the interval. A sample of results follows. Figure 4 shows the graphs for $a = 0.2$, $b = 0.2$, $\theta = \frac{3\pi}{4}$ when $n = 1$ (red), $n = 2$ (blue), $n = 10$ (green) and $n = 25$ (black).

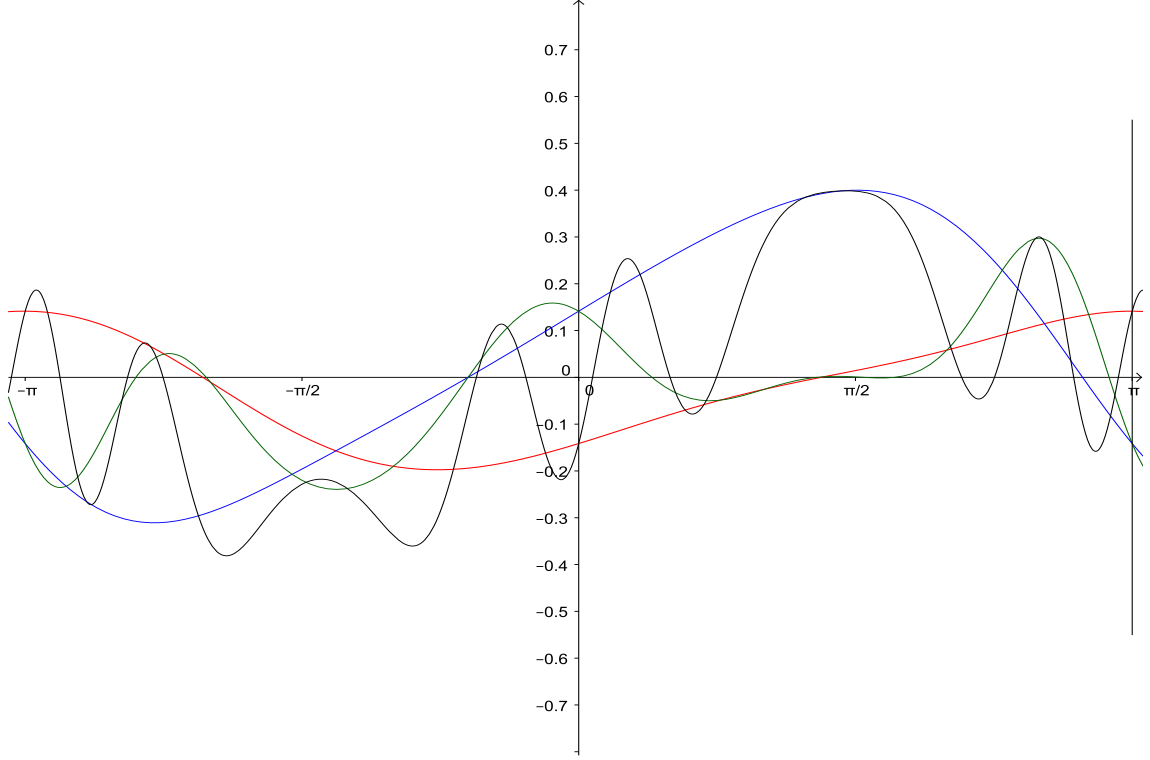


Fig.4 Graphs for $n = 1$ (red), $n = 2$ (blue), $n = 10$ (green) and $n = 25$ (black)

Table 1 gives ϕ values for $n = 1$ for $b = 0.2$ and various values of (a, θ) . Table 2 repeats Table 1 for $n = 2$. Values of ϕ are the zeros of the corresponding graphs.

Notes

1. The negative values in the tables refer to the anticlockwise ray; the positive to the clockwise ray. Note the antisymmetry in the values.
2. There were slight inaccuracies in the roots when the graphs were flat.
3. The values in the tables are for the sources in a representative plane as discussed in the Introduction. The results obtained for this plane can be applied to any other source by rotating the plane about the line OP.

| $a \backslash \theta$ | $-\frac{3\pi}{4}$ | $-\frac{\pi}{2}$ | $-\frac{\pi}{4}$ | $\frac{\pi}{4}$ | $\frac{\pi}{2}$ | $\frac{3\pi}{4}$ |
|-----------------------|---------------------------|---------------------------|--------------------------|--------------------------|---------------------------|---------------------------|
| 0.05 | -11.46^0 167.3^0 | -14.32^0 166.16^0 | -9.17^0 171.89^0 | -171.89^0 9.17^0 | -166.16^0 14.32^0 | -167.3^0 11.46^0 |
| 0.1 | -25.78^0 150.11^0 | -28.65^0 155.27^0 | -16.62^0 166.73^0 | -166.73^0 16.62^0 | -155.27^0 28.65^0 | -150.11^0 25.78^0 |
| 0.15 | -46.41^0 134.07^0 | -41.83^0 147.82^0 | -22.92^0 163.29^0 | -163.29^0 22.92^0 | -147.82^0 41.83^0 | -134.07^0 46.41^0 |
| 0.2 | -79.07^0 122.04 | -54.43^0 142.09^0 | -28.07^0 161.0^0 | -161.0^0 28.07^0 | -142.09^0 54.43^0 | -122.04^0 79.07^0 |
| 0.25 | -107.14^0 113.45^0 | -64.17^0 138.08^0 | -32.09^0 159.28^0 | -159.28^0 32.09^0 | -138.08^0 64.17^0 | -113.45^0 107.14^0 |
| 0.3 | -119.75^0 106.57^0 | -72.77^0 134.65^0 | -35.52^0 158.14^0 | -158.14^0 35.52^0 | -134.65^0 72.77^0 | -106.57^0 119.77^0 |
| 0.4 | -130.63^0 97.4^0 | -83.08^0 130.06^0 | -41.25^0 155.84^0 | -155.84^0 41.25^0 | -130.06^0 83.08^0 | -97.4^0 130.63^0 |
| 0.5 | -135.22^0 91.67^0 | -89.38^0 127.2^0 | -42.26^0 154.7^0 | -154.7^0 42.26^0 | -127.2^0 89.38^0 | -91.67^0 135.22^0 |
| 0.7 | -139.23^0 84.22^0 | -96.26^0 123.19^0 | -50.42^0 152.98^0 | -152.98^0 50.42^0 | -123.19^0 96.26^0 | -84.22^0 139.23^0 |
| 0.9 | -141.52^0 80.21^0 | -100.27^0 120.89^0 | -53.86^0 151.83^0 | -151.83^0 53.86^0 | -120.89^0 100.27^0 | -80.21^0 141.52^0 |

Table 1 Values of ϕ for $n = 1$

| $a \backslash \theta$ | $-\frac{3\pi}{4}$ | $-\frac{\pi}{2}$ | $-\frac{\pi}{4}$ | $\frac{\pi}{4}$ | $\frac{\pi}{2}$ | $\frac{3\pi}{4}$ |
|-----------------------|--------------------------|---------------------------|---------------------------|---------------------------|---------------------------|--------------------------|
| 0.05 | -172.46^0 9.74^0 | -166.73^0 14.32^0 | -166.45^0 10.6^0 | -10.6^0 166.45^0 | -14.32^0 166.73^0 | -9.74^0 172.46^0 |
| 0.1 | -168.45^0 18.9^0 | -157.56^0 29.79^0 | -150.11^0 22.64^0 | -22.64^0 150.11^0 | -29.79^0 157.56^0 | -18.9^0 168.45^0 |
| 0.15 | -165.58^0 27.78^0 | -151.26^0 46.98^0 | -138.08^0 37.82^0 | -37.82^0 138.08^0 | -46.98^0 151.26^0 | -27.78^0 165.58^0 |
| 0.2 | -163.87^0 35.81^0 | -147.25^0 65.89^0 | -130.06^0 90.81^0 | -90.81^0 130.06^0 | -65.89^0 147.25^0 | -35.81^0 163.87^0 |
| 0.25 | -162.72^0 42.97^0 | -144.39^0 83.08^0 | -124.33^0 132.35^0 | -132.35^0 124.33^0 | -83.08^0 144.39^0 | -42.97^0 162.72^0 |
| 0.3 | -161.57^0 49.27^0 | -142.09^0 94.54^0 | -120.32^0 138.95^0 | -138.95^0 120.32^0 | -94.54^0 142.09^0 | -49.27^0 161.57^0 |
| 0.4 | -160.43^0 59.01^0 | -139.23^0 105.71^0 | -114.31^0 144.39^0 | -144.39^0 114.31^0 | -105.71^0 139.23^0 | -59.01^0 160.43^0 |
| 0.5 | -159.28^0 65.32^0 | -136.94^0 111.15^0 | -110.58^0 147.25^0 | -147.25^0 110.58^0 | -111.15^0 136.94^0 | -65.32^0 159.28^0 |
| 0.7 | -158.14^0 73.06^0 | -134.65^0 116.31^0 | -105.71^0 149.54^0 | -149.54^0 105.71^0 | -116.31^0 134.65^0 | -73.06^0 158.14^0 |
| 0.9 | -157.56^0 77.35^0 | -132.93^0 119.18^0 | -102.56^0 150.69^0 | -150.69^0 102.56^0 | -119.18^0 132.93^0 | -77.35^0 157.56^0 |

Table 2 Values of ϕ for $n = 2$

5 Possible Application to Astronomy

The accepted model of the Milky Way galaxy is that there is a black hole at the centre, around which there is a densely distributed ball of stars with the rest of the stars lying in spiral arms in a disk which is approximately 1000 light years (ly) thick and 120000 ly in diameter. Our Sun lies in one of these arms around 25000 ly from the centre. The density of the star distribution in the outer regions of the disk is much lower than near the centre. As seen from the Earth there is a 'cloud' that can be seen in every direction in the disk plane. The present explanation of this cloud is that it is just the light of billions of stars. This may be the case but one should be open to another possibility viz that it may be the reflected light from a reflecting surface surrounding the Milky Way.

The first step in trying to prove that such a surface exists is to study objects which are known to be outside our galaxy. Clearly external galaxies are such objects and if such a surface exists these galaxies would be images of

the central core of our galaxy. Before we can use our model to test this idea, one needs a few preliminary results on galactic coordinates, great circles and how to obtain the angle of sight ϕ .

1. **Galactic Coordinates** Most star charts (for example [2]) give the position of a celestial object in terms of the Equatorial Coordinate System using Declination (Dec or δ) and Right Ascension (RA or α) which places the object on a celestial sphere as seen from the Earth. The Galactic Coordinate System uses the Sun as the origin, z-axis is perpendicular to the galactic plane and the x-axis points towards the centre of the galaxy. The objects on the celestial sphere are located using the **galactic latitude** b as elevation above the galactic plane and the **galactic longitude** l as the direction relative to the centre of the galaxy (i.e. the anticlockwise angle from the x-axis). Using spherical trigonometry, one can obtain the transformations of these coordinates into one another. Interested reader can find this on the internet. In particular [3] gives (l, b) for any given (α, δ) . A number of results is given in Table 3 for a few galaxies. Note that there may be slight errors as the author may have mixed the Epochs.
2. **Great Circles** Suppose a source of light S is located at (l, b) in galactic coordinates on the celestial sphere. Then the object of this source can be anywhere on the line of sight from the observer P to S ; in particular from a point where PS intersects the reflecting surface. This point is on the plane containing the lines PS and PO , where O is the centre of the reflecting spherical surface as well as the great circle formed where the plane intersects the reflecting surface. Point S is $(\cos b \cos l, \cos b \sin l, \sin b)$ in rectangular coordinates. Plane is

$$z = cy, \quad c = \frac{\sin b}{\cos b \sin l} = \frac{\tan b}{\sin l}.$$

This constant is given in Table 3 for a few galaxies. Figure 5 shows the planes in profile i.e. as they cut the yz-plane.

3. **Angle of sight ϕ** The angle of sight as defined in Section 2 is the angle that PS makes with \mathbf{i} (in this case $-\mathbf{i}$ which gives

$$\cos \phi = -\cos b \cos l.$$

The values of ϕ are also given in Table 3 for a few galaxies. Note that the sign of ϕ has been adjusted to correspond to the sign of b . The angles ϕ and the corresponding category 1 incident rays (i.e. for $n = 1$) are shown in Figure 6.

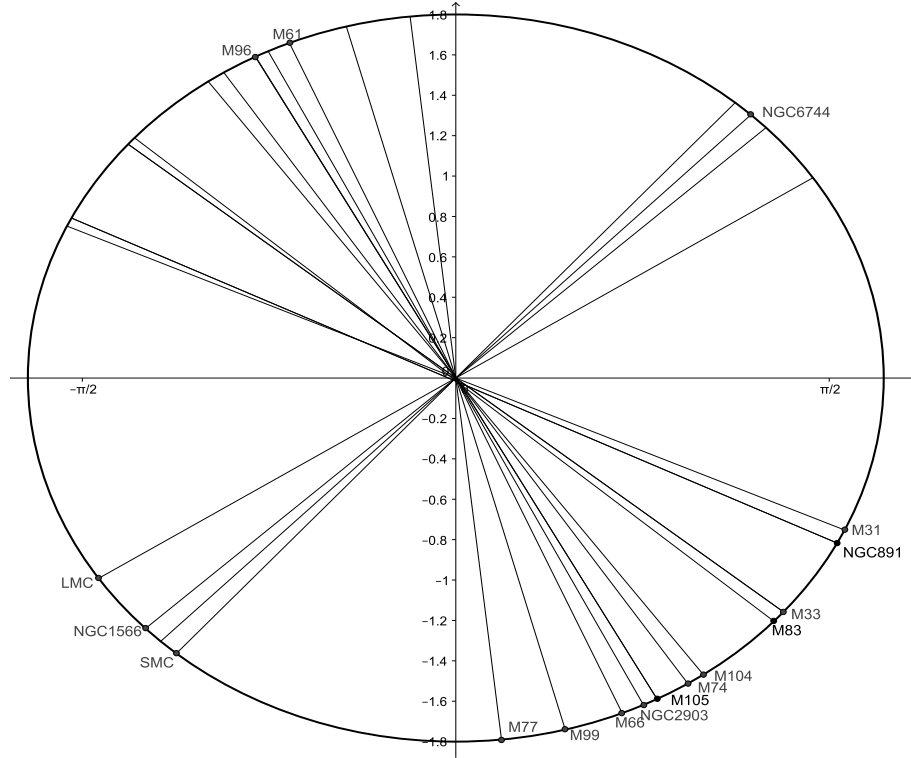


Fig.5 Planes of galaxies

Notes on Fig 6

1. Figure 6 was obtained after a number of attempts to place the observer P at different positions but failed to yield a common starting point for the incident rays like the dashed disc in the diagram.
2. When the desired effect was achieved, it was found that the observer's position (the Sun) is 0.2 from the centre (the circle has radius = 1) and about 0.4 from the centre of the dashed circle which would have to be the core of the galaxy i.e. the centre of the galaxy. If we take the distance of the Sun from the centre of the galaxy as 25000 ly then the radius of the spherical surface is approximately 62500ly.
3. One unexpected result shown by the diagram is that the centre of the galaxy is not the centre of the spherical surface. This perhaps introduces the possibility that the reflecting surface is ellipsoidal with the core of the galaxy at one focus. This will be looked at briefly in the next section.
4. Although the rays are shown on the same two dimensional diagram, they are in different planes as shown in Figure 5. The dashed disc

is actually a ball of diameter 12000 ly (approx) corresponding to the central bar of the galaxy whose half size is quoted between 3000 and 16000 ly.

5. The reconstruction of the images of the observed galaxies is hard as it requires a detailed knowledge of the distribution of stars along the whole 'incident' rays (see Figure 3)- not only the category 1 rays shown in Figure 6 but all other category rays. Another problem could be that our model assumes stationary sources and observers which is not true. For example, if the direct ray took 5000 years and the image ray took 100000 years, the stars position would be different now and when the image ray started. One has to remember also that the points and planes in our discussion are idealization of the actual points and planes which could be hundreds of light years across.

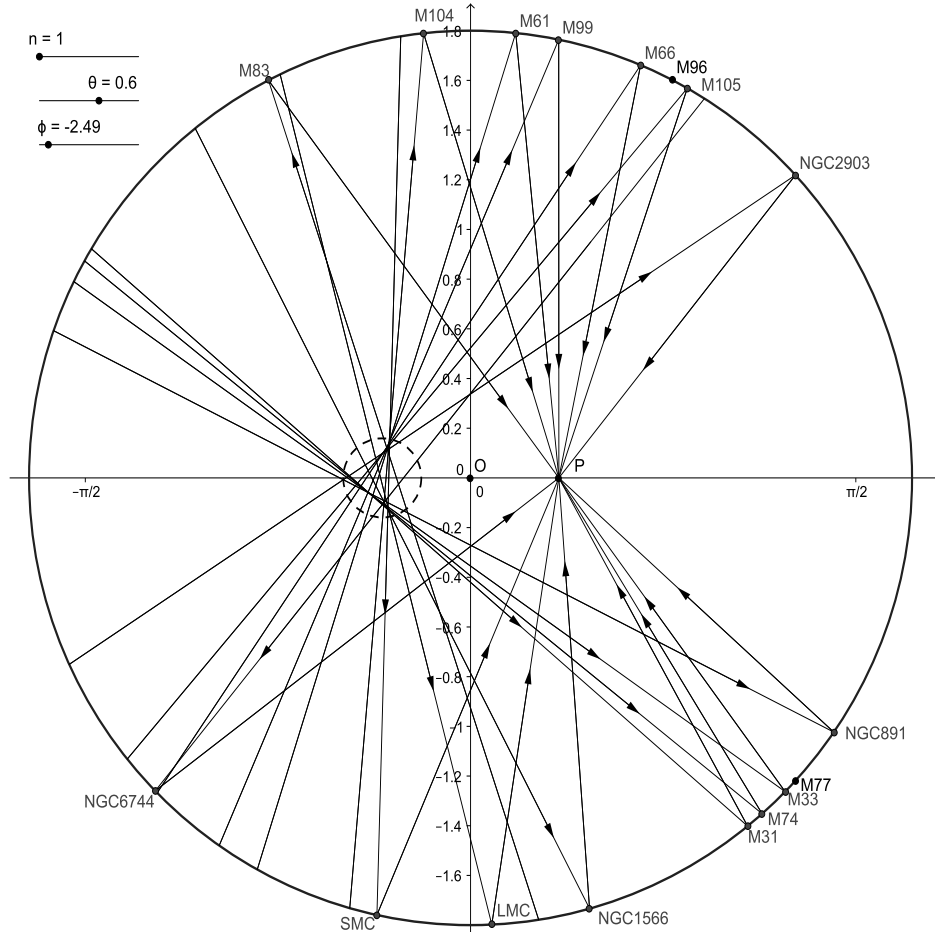


Fig.6 Possible sources for image galaxies

| <i>Galaxy</i> | l^0 | b^0 | c | ϕ^0 |
|----------------|--------|--------|-------|----------|
| <i>M31</i> | 121.17 | −21.58 | −0.46 | −61.23 |
| <i>SMC</i> | 302.81 | −44.33 | 1.16 | −112.81 |
| <i>M33</i> | 133.63 | −31.34 | −0.84 | −53.89 |
| <i>M74</i> | 138.62 | −45.71 | −1.55 | −58.4 |
| <i>NGC891</i> | 140.39 | −17.41 | −0.49 | −42.68 |
| <i>M77</i> | 172.11 | −51.93 | −9.31 | −52.36 |
| <i>NGC1566</i> | 264.3 | −43.4 | 0.95 | −85.86 |
| <i>LMC</i> | 280.46 | −32.89 | 0.66 | −98.77 |
| <i>NGC2903</i> | 208.72 | 44.55 | −2.05 | 51.32 |
| <i>M105</i> | 233.48 | 57.63 | −1.96 | 71.42 |
| <i>M66</i> | 241.93 | 64.41 | −2.37 | 78.27 |
| <i>M99</i> | 270.41 | 75.19 | −3.78 | 90.1 |
| <i>M96</i> | 234.45 | 57.02 | −1.89 | 71.55 |
| <i>M61</i> | 284.37 | 66.27 | −2.35 | 95.73 |
| <i>M104</i> | 298.46 | 51.16 | −1.41 | 107.39 |
| <i>M83</i> | 314.58 | 31.97 | −0.88 | 126.54 |
| <i>NGC6744</i> | 332.23 | −26.15 | 1.05 | −142.59 |

Table 3 Values of l , b , c , and ϕ for a few galaxies

6 Ellipsoidal Surface

In the last section it was indicated that, according to our model, the ‘centre’ of the galaxy doesn’t coincide with the centre of the spherical surface. One possible explanation is that the spherical surface is an approximation of an ellipsoidal surface. For example if we take

$$\frac{x^2}{(1.02)^2} + y^2 + z^2 = 1,$$

where the centre of the galaxy, the centre of the ellipsoid and the observer (the Sun) are on the $x - axis$, then the great circles discussed previously have to be replaced by ellipses

$$\frac{x^2}{(1.02)^2} + y^2 = 1.$$

This ellipse has semimajor axis = 1.02, semiminor axis = 1 and eccentricity $e = 0.196$. With the scaling in the last section these numbers become 63750ly and 62500ly respectively.

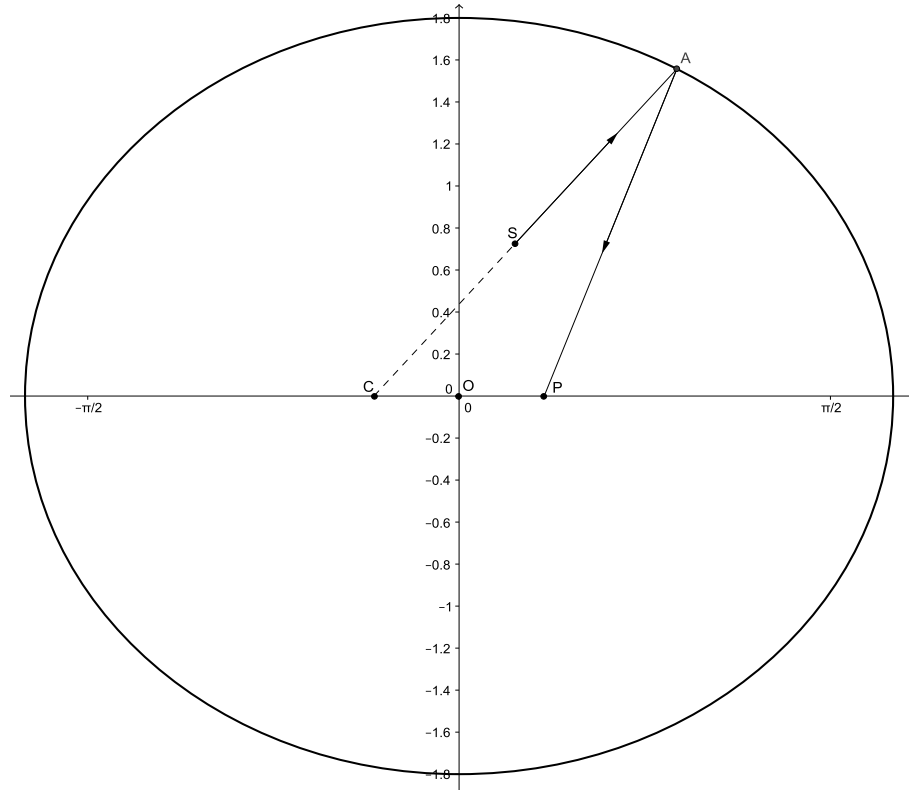


Fig. 7 Elliptical cross-section

Now the centre, C , of the galaxy would be at one focus (see Figure 7) and the Sun somewhere near the other focus P . One of the properties of the ellipse is that any ray starting at C will finish on reflection at P . If the source is at S then a ray SA which is an extension of CS will also finish at P . The normal to the surface bisects the angle $\angle CAP$. General ellipsoids are much more challenging and will not be attempted here.

7 Conclusion

This is an 'ideas' paper with the suggestion that there is a reflecting surface surrounding our Milky Way galaxy. The study looked at the surface as being spherical with a possibility that it may be ellipsoidal. If the surface exists, many mysteries encountered in astronomy at present can be explained using simple mathematics. If the surface is endowed with some properties then such results as red shifts and hence tremendous speeds can be explained. The hard task is to prove or disprove the existence of such a surface. An easy way is to dismiss it as absurd. In this paper a small step has been made towards the support of such a surface by showing that the observed

galaxies could be regarded as images of the core of our galaxy. Professional astronomers would have the resources to see whether these galaxies have the right profiles when the core of the Milky Way is cut by different planes.

REFERENCES

1. GeoGebra: www.geogebra.org
2. Wallace, K., Dawes, G., and Northfield, P.: Astronomy 2010 Australia, Quasar Publishing.
3. Equatorial to Galactic Coordinate Converter-FUSE:
fuse.pha.jhu.edu/support/tools/eqtogal.html